

## TECHNICAL NOTES

### Rectangular Capillaries for Capillary Zone Electrophoresis

Takao Tsuda,<sup>1</sup> Jonathan V. Sweedler, and Richard N. Zare\*

Department of Chemistry, Stanford University, Stanford, California 94305

#### INTRODUCTION

Capillary zone electrophoresis (CZE) is one of the most powerful separation techniques for the analysis of a wide variety of complex mixtures (1-4). The technique is capable of very high resolution; moreover, with CZE, it is possible to analyze nanoliter samples. In the past, separations in CZE have been almost exclusively performed in capillaries having circular cross sections with internal diameters between 2 and 200  $\mu\text{m}$ . The small size of the capillary allows extremely efficient heat dissipation, but as the capillary dimensions are increased beyond 100  $\mu\text{m}$ , a dramatic decrease in separation efficiency is observed. Joule heating, owing to the ionic current carried between the electrodes, can result in temperature gradients and subsequent density gradients and convection that increase zone broadening, affect electrophoretic mobilities, and even lead to boiling of the solvent (5). Consequently, CZE cannot be scaled to larger diameter capillaries, even with efficient cooling of the outside of the capillary with heat transfer fluids (6).

Furthermore, the path length available in such small circular capillaries limits the detection sensitivity. The ability to detect low concentration samples in a 50- $\mu\text{m}$  capillary is difficult, especially when using the very common technique of UV-vis absorbance.

Another inherent problem associated with conventional circular capillaries is the optical distortion caused by the curvature of the capillary walls. For example, the curvature at the solute-wall interface or at the wall-atmosphere interface will adversely affect refractive index or photodeflection measurements. It may also contribute to unwanted scattered light. In addition, when direct counting methods are employed, the curvature of the capillary walls can cause inaccurate counts.

This note describes studies on the use of transparent rectangular capillaries for CZE with dimensions ranging from 16 by 195  $\mu\text{m}$  to 50 by 1000  $\mu\text{m}$  with wall thicknesses from 20 to 50  $\mu\text{m}$ . Figure 1 shows a photomicrograph of the 50 by 1000  $\mu\text{m}$  i.d. capillary used in these studies (WRT5015, Wilmad Glass Co., Buena, NJ). As can be seen, the quality of the optical surfaces is excellent in the rectangular capillary. Because of the large height-to-width aspect ratio of a rectangular capillary, and hence extremely high surface-area-to-volume ratio, rectangular capillaries are extremely efficient at dissipating heat compared to conventional circular capillaries. Thus, larger volume rectangular capillaries can be used with comparable heat dissipation (7). In fact, the circular geometry of conventional capillaries is one of the worst possible configurations in terms of heat dissipation.

As an example illustrating the relative volumes of these capillaries, the typical injection volume is increased from a 2-nL injection for a 50  $\mu\text{m}$  circular capillary to 50 nL for a 50 by 1000  $\mu\text{m}$  capillary, both assuming a 1 mm long sample zone.

For almost all CZE injection methods, at least 1  $\mu\text{L}$  of analyte is required, even when the actual amount injected onto the capillary is only a few nanoliters (3, 8, 9). The large mismatch between injected amount and sample required is greatly reduced for these rectangular capillaries. In other words, no more analyte is required to perform the separation, even though the amount injected is much greater.

One of the greatest advantages to the rectangular geometry is that of detector sensitivity. For path-length-dependent detection schemes, such as UV-vis absorbance, optical rotation, and fluorescence, greater than an order of magnitude increase in concentration sensitivity can be achieved. In addition, the flat walls produce less optical distortion and scatter compared to the walls of circular capillaries. This is particularly important when on-column detection is based on refractive index, photodeflection, direct visualization, or particle counting.

The first use of a migration channel having a rectangular cross section for electrophoresis appears to be described by Tiselius (7). Some of the original isotachopheresis work was performed in rectangular separation channels (10, 11), and a combination isotachopheresis/capillary zone electrophoresis experiment using such a rectangular separation channel has been described (12). These channels were usually made in-house from a block of plastic, with typical sizes being much larger than the rectangular capillaries described here. In addition, Hjertén has mentioned the use of transparent rectangular separation channels for capillary electrophoresis (13). Jansson, Emmer, and Roeraade (14) recently published the results of several theoretical calculations on heat dissipation and separation time using rectangular capillaries with dimensions optimized for CZE, and as expected, thin rectangular channels are shown to be greatly advantageous in minimizing the effects of Joule heating. Because the advantages of the rectangular geometry in terms of heat dissipation have been well treated by a variety of authors (14-16), a similar discussion is not repeated here.

Other advantages of the rectangular structure have been investigated for use in gas chromatography (17-19) and liquid chromatography (20), although these techniques do not require the heat dissipating abilities offered by these capillaries. In LC, the ends (corners) of the rectangular capillaries cause a significant decrease in resolution. It might be wondered if this deleterious effect overwhelms the possible gain from sample throughput in CZE. Fortunately, the electroosmotic flow profile in CZE, as opposed to the laminar flow profile in LC, greatly reduces the effects of the ends of the separation channel. We show high-resolution separations are possible in CZE with capillaries of various rectangular cross sections.

#### EXPERIMENTAL SECTION

**Apparatus and Procedure.** The rectangular capillaries (20 by 200, 30 by 300, 50 by 500 and 50 by 1000  $\mu\text{m}$ , as well as the square capillaries of 50 by 50  $\mu\text{m}$  and 100 by 100  $\mu\text{m}$ ) are from Wilmad Glass Co. (Buena, NJ) and are marketed as microvials. All are borosilicate glass and are not available with any protective

<sup>1</sup> On sabbatical leave, permanent address is the Department of Applied Chemistry, Nagoya Institute of Technology, Gokiso, Showa, Nagoya 466, Japan.

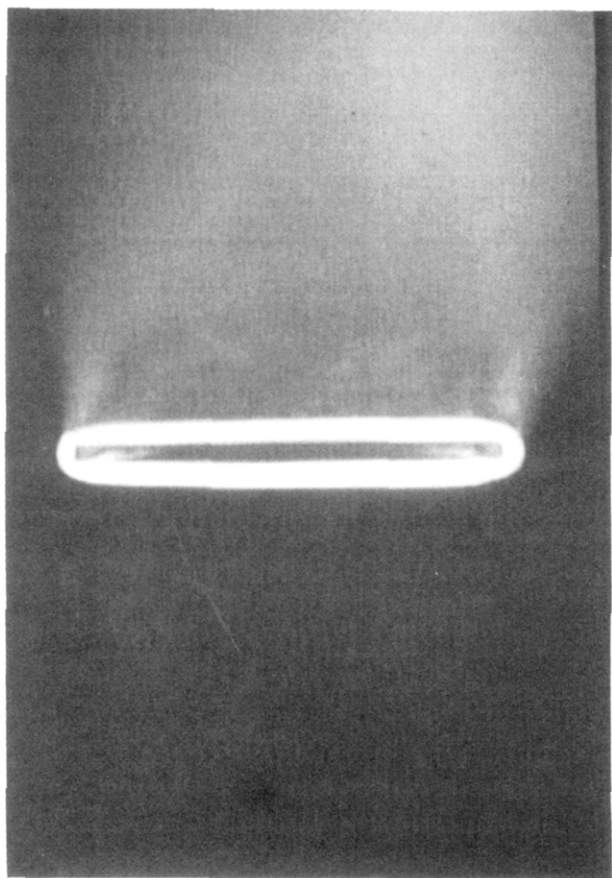


**Figure 1.** Photomicrograph showing the cross section of the 50 by 1000  $\mu\text{m}$  i.d. rectangular capillary with 50  $\mu\text{m}$  walls.

coatings (e.g., polyimide). A significant disadvantage of the Wilmad Glass Co. capillaries is their thin walls; in all cases, the available wall thickness is equal to the width of the narrowest dimension—for example, 20 by 200  $\mu\text{m}$  capillaries have 20  $\mu\text{m}$  walls, and 50 by 1000  $\mu\text{m}$  capillaries have 50  $\mu\text{m}$  walls. Care must be taken to avoid breaking these capillaries.

In most cases, the capillary diameters are reported as specified by Wilmad Glass; however, we have measured the diameters by use of a calibrated video-microscope system. The system consists of a Nikon SMZ-2T stereoscopic microscope (Nikon Co., Tokyo, Japan) equipped with a Sony DXC-101 color video CCD camera (Sony Co. of America, Park Ridge, NJ) calibrated with a Nikon 1 mm stage micrometer. For the smaller diameter capillaries, there are significant differences between our measured values and the values specified by Wilmad Glass; in the case of the particular 30 by 300  $\mu\text{m}$  capillary tested, the measured inner diameter is 27 by 340  $\mu\text{m}$ , and for the 20 by 200  $\mu\text{m}$  capillary tested, 16 by 195  $\mu\text{m}$ . Thus, for the smaller capillaries, the measured sizes are reported.

An ISCO CV4 capillary electrophoresis UV-vis absorbance detector is used for detection, with the detector output plotted on a strip chart recorder. Because the capillaries are fragile and not so flexible as coated circular capillaries, the detector is modified to allow the capillaries to pass through the unit without any bends. This necessitated removing the cover of the detector, cutting a channel in the optical compartment of the system, and modifying the capillary cell holder to allow the larger 1000  $\mu\text{m}$  capillaries to be used. For the 1000  $\mu\text{m}$  path length studies, the modified ISCO slits are used (50 by 100  $\mu\text{m}$ ). For the other studies, the slit assembly is removed from the capillary holder, and individual slits (either 50 by 800  $\mu\text{m}$ , Yokogawa Electric Co., Tokyo, or 50 by 300  $\mu\text{m}$ , Beckman Instruments, Inc.) are manually positioned and glued onto the rectangular and square capillaries in the cell housing before mounting the capillaries into the absorbance detector.

The rest of the system is similar to previous systems constructed in our laboratory (21, 22). The injection end of the capillary is connected to high voltage, while the detector end is held at ground.

**Table I.** Efficiency and Separation Conditions of the Pyridoxine Peak for a Variety of Capillary Cross-Sectional Geometries

capillary size, $\mu\text{m}$	$L_{\text{total}}$ , cm	$L_{(\text{inj.}-\text{det.})}$ , cm	applied voltage, kV	current, $\mu\text{A}$	$N$
			Round		
51	53	34	15	27	$2.1 \times 10^5$
			Square		
50 by 50	60	43	15	39	$2.8 \times 10^5$
103 by 108	65	48	12	91	$1.3 \times 10^5$
			Rectangular		
16 by 195	53	34	12	27	$1.6 \times 10^5$
27 by 340	83	63	15	62	$2.1 \times 10^5$

The current through the capillary is monitored as a potential drop across a 10-k $\Omega$  resistor on the ground side of the circuit. The capillary and injector system are enclosed in an interlocked Plexiglas box to prevent exposure to high voltage.

Injection is performed either by gravity or by pressurized flow using a split injection technique (23, 24). For the smaller capillaries, gravity injection yields high-quality separations. Because the cross-sectional area is so large for the 50 by 1000  $\mu\text{m}$  capillaries, the resistance to fluid flow is small. In this case, the typical gravity and electrokinetic injection methods fail to give reproducible, high-efficiency separations, even when care is used to adjust the inlet and outlet reservoir heights and to transfer the capillaries from the buffer to sample reservoirs. Thus, a split injection method is employed.

The split flow technique involves using an HPLC pump (Beckman Solvent Delivery Module 112) with an HPLC injector (Rheodyne Model 7410) and a 1, 5, or 10  $\mu\text{L}$  sample injection loop. A junction has been constructed that allows approximately 1% of the output of the HPLC capillary to enter the rectangular capillary and 99% to flow to a waste container. Samples are introduced into the stream using the injector, and again, about 1% enters the rectangular capillary. The system allows automated, reproducible injections for an extremely wide variety of capillary sizes and shapes (24). In the current system, some dilution of the sample occurs between the HPLC injector and the CZE capillary. Consequently, the concentration of the analyte as it is injected onto the column is lower by a factor of approximately 8 than the concentration introduced into the injector. Because this is a limitation of the current injection system and not the rectangular capillary, the estimated concentrations of the analyte as it enters the rectangular capillary are used throughout this report.

**Reagents.** Dansyl-L-valine, dansyl-L-serine, dansyl-L-aspartic acid, dansyl-L-cysteic acid, and pyridoxine were purchased from Sigma and used without further purification. The water used to prepare all solutions was freshly distilled and deionized with a water purifier (Model LD-2A coupled with a Mega-Pure Automatic Distiller, Corning Glassworks). The supporting electrolyte for all experiments was 5 mM phosphate buffer (pH 6.8) made from a mixture of  $\text{NaH}_2\text{PO}_4$  (Mallinckrodt) and  $\text{Na}_2\text{HPO}_4$  (J. T. Baker) with 5% ethylene glycol (Mallinckrodt) added to enhance separations.

## RESULTS AND DISCUSSION

One of the most important questions concerning the use of rectangular capillaries for CZE involves the ability of the system to perform high-efficiency separations: i.e., what are the effects of the "corners" of the capillary on zone spreading? In order to determine the effects of capillary geometry on separation efficiency, a variety of cross-sectional geometry capillaries are evaluated, with pyridoxine used as a test compound. Table I summarized the electrophoretic conditions for the 27 by 340  $\mu\text{m}$  and 16 by 195  $\mu\text{m}$  rectangular borosilicate capillaries, the 52 by 52 and 103 by 108  $\mu\text{m}$  "square" borosilicate capillaries, and the 51  $\mu\text{m}$  round fused silica capillary (Polymicro, Phoenix, AZ), with the electropherograms ob-

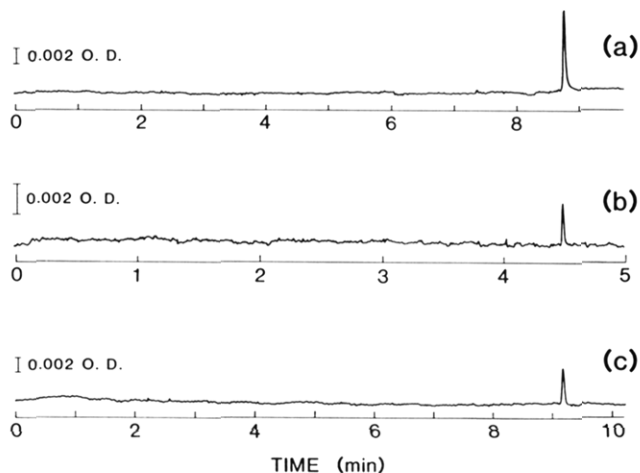


**Figure 2.** CZE electropherograms of pyridoxine for rectangular, square and round cross-sectional geometry capillaries: (a) 27 by 340  $\mu\text{m}$  rectangular; (b) 52  $\mu\text{m}$  square; and (c) 51  $\mu\text{m}$  round. The separation conditions and peak efficiencies are listed in Table I.

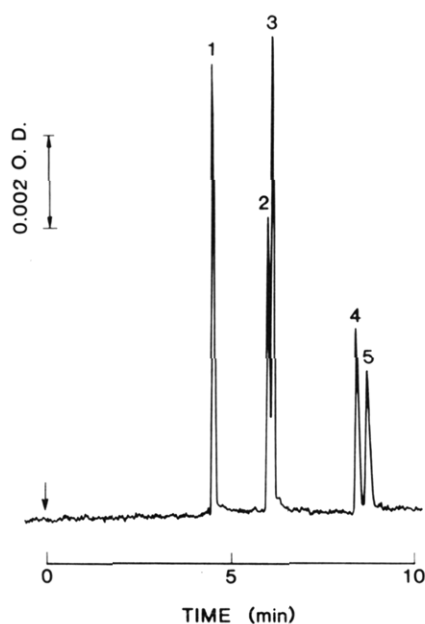


**Figure 3.** CZE electropherogram of (1) pyridoxine, (2) dansyl-L-valine, (3) dansyl-L-serine, (4) dansyl-L-aspartic acid, and (5) dansyl-L-cysteic acid, each injected at  $1.3 \times 10^{-5}$  M. The separation conditions are a 57 cm long and 50 by 1000  $\mu\text{m}$  i.d. capillary, 10 kV applied voltage, 132  $\mu\text{A}$  current, and 310 nm detection.

tained with the 27 by 340  $\mu\text{m}$ , the 52 by 52  $\mu\text{m}$  and the 51  $\mu\text{m}$  round capillaries shown in Figure 2. In all cases, sample injection is accomplished by using approximately a 1 s, 4 cm displacement gravity injection of between  $10^{-2}$  and  $10^{-3}$  M pyridoxine. The observed current and separation time depend on the capillary geometry and differ widely for each configuration. The efficiencies for the pyridoxine peaks listed in Table I are calculated directly from the electropherograms (25) and are not corrected for different zone velocities (26). In all cases,  $N$  is  $>130\,000$ ; the efficiency is highest for the smaller 52 by 52  $\mu\text{m}$  square and 27 by 340  $\mu\text{m}$  rectangular capillaries. The 27 by 340  $\mu\text{m}$  capillary, with an 18% smaller cross-sectional area and a 74% greater surface area than the 103 by 108  $\mu\text{m}$  capillary, produces a much higher efficiency electropherogram.

The electropherograms shown in Figure 2 demonstrate that rectangular capillaries may indeed be used for CZE; there is no indication that the corners of the capillary degrade the separation. Further studies will determine the effects of

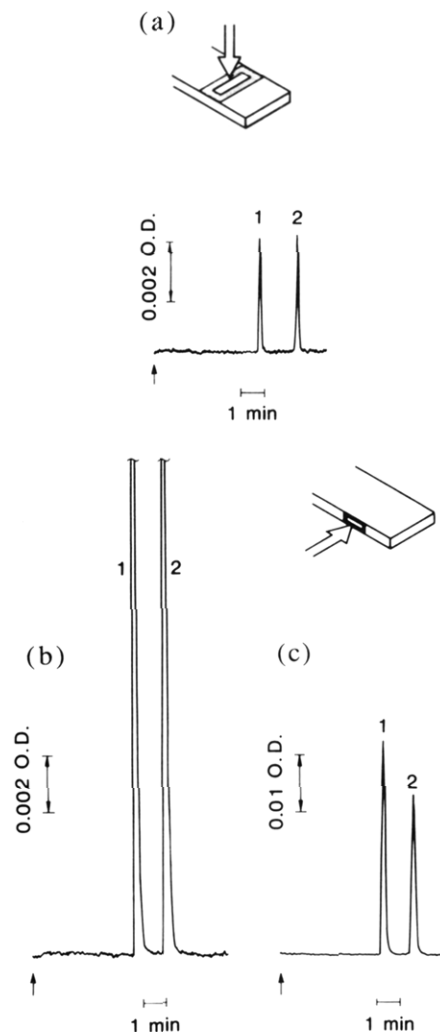


**Figure 4.** CZE electropherogram of (1) pyridoxine and (2) dansyl-L-serine, each at  $4.2 \times 10^{-5}$  M, using two different detector arrangements of the rectangular capillary in the UV-vis absorbance detector. In part a, the capillary was positioned so that detection was across the 50  $\mu\text{m}$  axis of the capillary, and in parts b and c, across the 1000  $\mu\text{m}$  axis of the capillary. In part b, the electropherogram is recorded by using the same detector sensitivity as in part a and the peaks are off-scale, while in part c, the sensitivity has been reduced by a factor of 5.

capillary geometry on flow profile as well as optimum separation conditions.

While CZE can achieve high resolution separations, increasing the size of a conventional round capillary beyond 100  $\mu\text{m}$  inside diameter normally greatly degrades the separation efficiency. One of the larger potential benefits of the rectangular capillaries is in increasing the sample size using wide separation channels. As a test of this, separations in a 50 by 1000  $\mu\text{m}$  rectangular capillary were undertaken, in this case, using the split injection technique. Figure 3 demonstrates a moderately high-resolution separation of four dansyl amino acids and pyridoxine (each at  $1.3 \times 10^{-5}$  M) using the 50 by 1000  $\mu\text{m}$  capillary. The number of theoretical plates varies from 20 000 to 60 000 for these substances. While not high by CZE standards, much of the width of these peaks may be attributed to the width of the injection zone.

In order to determine the gain in sensitivity obtained with the increased path length of the rectangular capillary, the sensitivity of the system is determined by using two different detection geometries for the 50 by 1000  $\mu\text{m}$  capillary: a 50  $\mu\text{m}$  path length across the short axis of the separation channel, and a 1000  $\mu\text{m}$  path length across the long axis of the capillary. Pyridoxine and dansyl-L-serine (each at  $4.2 \times 10^{-4}$  M) are used

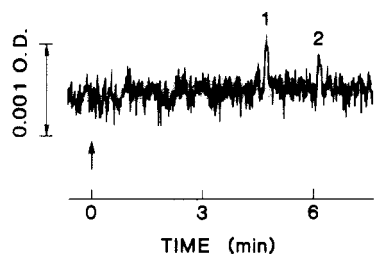


**Figure 5.** CZE electropherogram of (1) pyridoxine and (2) dansyl-L-serine with the conditions as in Figure 4b,c, each at a concentration of  $8 \times 10^{-7}$  M.

as the test mixture. Parts a and b of Figure 4 show the absorbance electropherogram obtained across the 50  $\mu\text{m}$  path length and across the 1000  $\mu\text{m}$  path length, respectively. In the latter case, the peak is off-scale, and a lower sensitivity trace is shown in Figure 4c. The applied voltage was 7.9 kV in part a and 9 kV in parts b and c, with a capillary length of  $\approx 60$  cm and a current of  $\approx 110$   $\mu\text{A}$ . The current density of 110  $\mu\text{A}$  is similar to a current of 4  $\mu\text{A}$  in a 50  $\mu\text{m}$  circular capillary. As can be seen in this figure, approximately a 15-fold increase in sensitivity is gained by the longer path length.

The improvement in detection sensitivity from the cell path length increase is most pronounced when the concentration of sample is low. For instance, when the concentration of sample is just sufficient to be detectable in a 50  $\mu\text{m}$  path length rectangular capillary, then a gain of nearly 20 is observed by employing a rectangular capillary with a path length of 1000  $\mu\text{m}$ . Figure 5 shows an electropherogram obtained at  $8 \times 10^{-7}$  M in both pyridoxine and dansyl-L-serine—just above the limit of detection. The sensitivity of the system is reduced compared to conventional systems; 310-nm light is used instead of the optimum wavelength ( $\approx 250$ –280 nm) because of the high absorbance of the borosilicate glass capillary walls for the shorter wavelengths.

### CONCLUSIONS

This study demonstrates the feasibility and the advantages of rectangular capillaries for CZE. The separations shown in this report are more than adequate for most applications, but the peak widths are wider than common for the highest resolution CZE separations obtainable with circular cross section capillaries. It is expected that by optimizing the separation conditions and the injection system, the separation efficiency can be further improved, especially for the larger rectangular capillaries. In addition, rectangular fused silica capillaries are being constructed with polyimide coatings, thus alleviating the problems of capillary fragility and ultraviolet absorbance.

The rectangular cross section allows a very significant increase in the sensitivity of UV-vis absorbance and other path-length-dependent detection methods. In addition, the reduction of optical distortion and scatter by the flat capillary walls is very important for a number of additional optical detection schemes. For example, the ability to image the capillary without distortion allows extremely accurate flow profiles to be obtained for sample zones during the CZE separation (27); thus fundamental studies of the factors affecting zone broadening and zone profiles can be performed. Another major advantage is the ability to scale the injection size as needed by making the capillary wider. If larger scale (preparative) separations are needed, one can envision separation channels formed between two flat plates separated by

a spacer, with the ultimate limits of volume limited by geometrical constraints.

One of the most exciting possibilities of these flat separation channels is the ability to perform two-dimensional separations, with one applied force being the electric field along the capillary, the second force being applied across the separation channel, with the sample zones detected by use of a multi-channel array detector. Many gradients can be envisioned, including pH, gravity, and magnetic field. Such a spatial two-dimensional (2D) separation is similar in principle to the techniques of field flow fractionation (28, 29) and free-flow cell electrophoresis (30) in terms of the use of two orthogonal separation forces. The resolution of 2D CZE is expected to be higher than possible with the other techniques because of the narrower zone profile of electroosmotic flow compared to laminar flow.

### ACKNOWLEDGMENT

The many useful discussions and comments of Steven L. Pentoney, Jr., and Xiaohua Huang are greatly appreciated.

### LITERATURE CITED

- (1) Jorgenson, J. W.; Lukacs, K. D. *Science* **1983**, *222*, 266–272.
- (2) Gordon, M. J.; Huang, X.; Pentoney, S. L.; Zare, R. N. *Science* **1988**, *242*, 224–228.
- (3) Ewing, A. G.; Wallingford, R. A.; Olefirowicz, T. M. *Anal. Chem.* **1989**, *61*, 292A–303A.
- (4) Karger, B. L.; Cohen, A. S.; Guttman, A. J. *Chromatogr.* **1989**, *492*, 585–614.
- (5) Roberts, G. D.; Rhodes, P. H.; Snyder, R. S. *J. Chromatogr.* **1989**, *480*, 35–67.
- (6) Roach, M. C.; Gozel, P.; Zare, R. N. *J. Chromatogr.* **1983**, *426*, 129–140.
- (7) Tiselius, A. *Trans. Faraday Soc.* **1937**, *33*, 524–530.
- (8) Schwartz, H. E.; Melera, M.; Brownlee, R. G. *J. Chromatogr.* **1989**, *480*, 129–137.
- (9) Rose, D. J.; Jorgenson, J. W. *Anal. Chem.* **1988**, *60*, 642–648.
- (10) Ryšlavý, Z.; Boček, P.; Deml, M.; Janák, J. *J. Chromatogr.* **1977**, *144*, 17–25.
- (11) Boček, P.; Deml, M.; Janák, J. *J. Chromatogr.* **1975**, *106*, 283–290.
- (12) Gebauer, P.; Deml, M.; Boček, P.; Janák, J. *J. Chromatogr.* **1983**, *267*, 455–457.
- (13) Hjerfén, S.; Elenbring, K.; Sedzik, J.; Vaitcheva, L. 6th International Symposium of Isotachophoresis and Capillary Zone Electrophoresis, September 21, 1988, Vienna, Austria.
- (14) Jansson, M.; Emmer, A.; Roeraade, J. *HRC CC, J. High Resolut. Chromatogr. Chromatogr. Commun.* **1989**, *12*, 797–801.
- (15) Coxon, M.; Binder, M. J. *J. Chromatogr.* **1975**, *109*, 43–50.
- (16) Brown, J. F.; Hinckley, J. O. N. *J. Chromatogr.* **1975**, *109*, 225–231.
- (17) Papendick, H.-D.; Baudisch, J. *J. Chromatogr.* **1978**, *122*, 443–450.
- (18) Sandra, P.; Verzele, M. *HRC CC, J. High Resolut. Chromatogr. Chromatogr. Commun.* **1980**, *3*, 253.
- (19) Martin, M.; Jurado-Baizaval, J.-L.; Guiochon, G. *Chromatographia* **1982**, *16*, 98–102.
- (20) Martin, M.; Jurado-Baizaval, J.-L.; Guiochon, G. *C. R. Acad. Sci., Ser 2* **1982**, *295*, 579–581.
- (21) Huang, X.; Luckey, J.; Gordon, M.; Zare, R. N. *Anal. Chem.* **1989**, *61*, 766–770.
- (22) Gozel, P.; Gassmann, E.; Michelson, H.; Zare, R. N. *Anal. Chem.* **1987**, *59*, 44–49.
- (23) Tsuda, T.; Novotny, M. *Anal. Chem.* **1978**, *50*, 271–275.
- (24) Tsuda, T.; Zare, R. N. Unpublished results.
- (25) Jorgenson, J. W.; Lukacs, K. D. *Anal. Chem.* **1981**, *53*, 1298–1302.
- (26) Huang, X.; Coleman, W. F.; Zare, R. N. *J. Chromatogr.* **1989**, *480*, 95–110.
- (27) Jones, G. C.; Tsuda, T.; Zare, R. N. Unpublished results.
- (28) Caldwell, K. D. *Anal. Chem.* **1988**, *60*, 959A–971A.
- (29) Giddings, J. C. *Anal. Chem.* **1981**, *53*, 1170A.
- (30) Hannig, K. *Electrophoresis* **1982**, *3*, 235–243.

RECEIVED for review May 25, 1990. Accepted June 5, 1990. T.T. thanks the Ministry of Education, Japan, for support during his sabbatical leave. J.V.S. thanks the National Science Foundation for a postdoctoral fellowship, administered under NSF CHE-8907446. The authors gratefully acknowledge the financial support of Beckman Instruments, Inc.